Optimal capacity threshold for reversible watermarking using score function

Chaiyaporn Panyindee
Department of Computer Engineering, Faculty of Engineering, Rajamangala University of Technology Rattanakosin,
Nakhon Pathom, Thailand

Article Info	ABSTRACT
	Histogram shifting is an important technique of reversible watermarking, which can embed large payloads into digital images with low distortion. The technique must determine two threshold values to achieve the lowest possible distortion. Appropriate threshold values might be found by iterative methods, but it is computationally inefficient when the payloads are high and varied. In this paper, we show that the optimal threshold values lie on a straight line and occur at the boundary of the payload-satisfying region. Moreover, we propose a high performance algorithm to approximate the optimal threshold values. Under the same image quality, experimental results indicate that the proposed scheme could get closer threshold values to the optimal threshold values, compared to previous work. Therefore, it requires a smaller number of iterations to obtain the desirable threshold values. *This is an open access article under the [CC BY-SA](#) license.*

Corresponding Author:

Chaiyaporn Panyindee
Department of Computer Engineering, Faculty of Engineering
Rajamangala University of Technology Rattanakosin
Nakhon Pathom, 73120, Thailand
Email: Chaiyaporn.pan@rmutr.ac.th

1. INTRODUCTION

Reversible watermarking is a data hiding technique developed for various purposes such as protecting product authentication, securing transfer of sensitive data, and database management. Reversible watermarking is a technique by which host images can be totally recovered after data extraction. Since the late 1990s, several reversible watermarking methods have been presented [1]–[4] and improved in order to increase the efficiency of the technique. Improvements include increasing the embedding capacity, decreasing image degradation, and reducing complexity of the algorithm. Some of the most popular techniques, which have been improved continuously, are integer wavelet transformation (IWT) [3]–[7], difference expansion (DE) [8]–[13], sorting [14]–[24], prediction-error expansion (PEE) [25]–[33] and histogram shifting (HS) [34]–[36].

DE technique [8] was first presented in 2003, uses the 1-D Haar wavelet transformation. This involves decomposing image data into low pass and high pass images. Bit shifting also occurs, as it applies to the pixel pair difference on the high pass image. This technique leaves vacant space in the least significant bit (LSB) so that more bits can be embedded into the image data. However, this technique suffers from high distortion and low embedding capacity.

In 2004, the PEE technique [25] was introduced, which is sometimes considered generalized DE. It dramatically decreases image distortion because PE values have small magnitudes compared to DE values. However, all of these previous works rely on the compression tool's capability of compressing auxiliary information, which is then sent to a decoder for image recovery. The binary location map is one of the auxiliary

information tools used to locate embedded pixels in an image. Many researchers have tried to reduce the map size by adjusting the proportion between 0 and 1 on the map.

The HS technique [34] was introduced in 2006, which pixel values want to be shifted between the peak and the zero frequency histogram bin in order to embed information bits to mode-value-pixels. Since the use of number of mode-value pixels is limited, payload carrying capability is also limited. Thodi and Rodriguez [26] presented algorithms when applied HS to prediction error histogram shifting (or called PEHS), helping to decrease distortion and increase efficiency of compression tools. Instead of using HS for embedding, It has been used to control a distortion caused by PEE. They introduced an adjusting map called the overflow map. The map is a well compressed, by-product of HS. The algorithms are well accepted and have been widely used in reversible watermarking work since then. In 2009, the algorithm [11] improved on PEHS [26] by reducing the size of overflow map and redesigning the algorithm. In later years, a mathematical model [27] was applied, based on [11], to determine proper capacity parameters using in the PEHS method in order to minimize image degradation.

We introduced a novel and simple algorithm for finding capacity threshold values which minimize a modified image's distortion. A demonstrated scheme is simple and does not require a convex optimization solver (CVX) [37] used as in [27]. Instead, the threshold values can be evaluated directly from image data. Experimental results show that the scheme obtains threshold closer values to the optimal threshold values and results in a lower image degradation than previous schemes.

The rest of the paper is arranged as follows. In section 2, we discuss a model for prediction-error distribution and an image distortion optimization problem. In section 3 we describe the proposed method. In section 4 we show the experimental result. Concluding remarks are given in the last section.

2.   OPTIMIZATION OF IMAGE DEGRADATION

Among the many techniques that have been used together with PEE based reversible watermarking is the HS technique. The HS technique is popular, efficient and has low distortion. An algorithm [26] combined HS and PEE which could be referred to as PEHS. This technique divides the histogram into two separate sections. The first section is the inner region $[T_n, T_p]$, considered the expansion embedding part, where T_n is the non-positive integer threshold value ($T_n \in \mathbb{Z}$: $T_n \leq 0$) and T_p is the non-negative integer threshold value ($T_p \in \mathbb{Z}$: $T_p \geq 0$). The second one is the outer shifting region $(-\infty, T_n) \cup (T_p, \infty)$. This part does not carry any hidden data and the shifting method causes less distortion than expansion.

In the existing reversible image watermarking schemes, most iterative fine-tuning is to acquire optimal inner and outer region parameters that would result in the least amount of distortion. For example, algorithm [11], the first iteration starts at $T_p=0$ and $T_n=0$. The best values of the thresholds are determined by increasing T_p and decreasing T_n until the bins in the inner region provide enough space for the payload. Example path of shifting T_p and T_n in the second iteration is $T_p=0$ and $T_n=-1$, the third iteration is $T_p=1$ and $T_n=-1$, the fourth iteration is $T_p=1$ $T_n=-2$ and the fifth iteration is $T_p=2$ and $T_n=-2$. However, sometimes optimal values are not found. These methods generally require many iterations, especially when payloads are high. We also found that expanding the T_p and T_n range allows for more payloads to be embedded, but results in lower peak signal-to-noise ratio (PSNR).

A well-known fact about PE histogram is that it is a Laplacian-like distribution centered at zero. The Laplace distribution is also called the double exponential distribution. A better predictor provides a sharper Laplacian shape in general. In this field, the development and design of new predictors continues to be popular in order to increase efficiency for data embedding. The probability density function of Laplace has been used [27] to model the distortion and capacity functions. Thus, a capacity-distortion optimization function (CDO) can be transformed to be convex, which permits efficient solutions by using a convex optimization tool, e.g. CVX [37].

Referring to model [27], an optimization problem can be written as follows:

$$\begin{aligned} &min\ F(t_p, t_n) \\ &subject\ to\ C(t_p, t_n) \geq \tau \end{aligned}$$

(1)

where τ is a required payload. t_p is a non-negative real number ($t_p \in \mathbb{R}$: $t_p \geq 0$) and t_n is a non-positive real number ($t_n \in \mathbb{R}$: $t_n \leq 0$). Here $F(t_p, t_n)$ is continuous distortion function representing an estimated probability of distortion occurred in each pixel when using the threshold given by the inner product of $h(x)$ and $p(x)$:

$$\begin{aligned} F(t_p, t_n) &= \int_{-\infty}^{\infty} h(x)p(x)dx \\ &= (b - 0.5)t_n e^{t_n/b} - (b^2 - 0.5b + 0.25)e^{t_n/b} \\ &\quad -(b - 0.5)t_n e^{-t_p/b} - (b^2 + 0.5b - 0.25)e^{-t_p/b} \\ &\quad + 2b^2 + 0.5 \end{aligned}$$

(2)

The Laplace probability density function is $p(x)=(1/2b)e^{-|x|/b}$. This distribution is characterized by scale parameter $b=(1/N)\sum_{i=1}^{N}|pe_i|$ which has to be greater than zero. The prediction-error, pe_i, is the difference between the original value and the predicted value. N is the total number of prediction-errors. In (3) defines $h(x)$ a histogram shifting distortion function. There are three different defining sections in the function. The first is the expansion embedding distortion, and the rest are the shifting distortion.

$$h(x) = \begin{cases} (x + E[\{0,1\}])^2 & if\ x \in [t_n, t_p] \\ (t_p + 1)^2 & if\ x \in (t_p, \infty) \\ t_n^2 & if\ x \in (-\infty, t_n) \end{cases} \tag{3}$$

The expected value of data bit to be embedded is $E[\{0, 1\}]$. The possible bit values are 0 and 1 whose probabilities are equal. Thus $E[\{0, 1\}] = 0.5$. $C(t_p, t_n)$ is the continuous capacity function which represents an estimated embeddable capacity when using thresholds defined by (4):

$$C(t_p, t_n) = N - (N/2)(e^{t_n/b} + e^{-t_p/b}) \tag{4}$$

let us then calculate the first partial derivative of the distortion function $F(t_p, t_n)$ and the capacity function $C(t_p, t_n)$ with respect to t_p and t_n. The first partial derivatives of the distortion function and of the capacity function with respect to t_p are both greater than zero $Ft_p(t_p, t_n)>0$ when $b>(2t_p+1)/(4+4t_p)$ and $Ct_p(t_p,t_n)>0$. Similarly, the first partial derivative of both functions with respect to tn are less than zero $Ft_n(t_p, t_n)<0$ when $b>(2t_n+1)=4\ t_n$ and $Ct_n(t_p, t_n) < 0$. The signs of derivatives imply that the distortion function and the capacity function are increasing on $t_p \in (0, \infty)$ and decreasing on $t_n \in (-\infty, 0)$ if b is greater than 0.5. In general, most natural images have a scale parameter greater than 0.5.

From the argument above, the minimum solution of the optimization problem must be located at the boundary of the feasible region which included the endpoints $min\{F(t_p, t_n) \mid C(t_p, t_n) = \tau\}$ of the boundary of the region. We can solve this optimization problem with equality constraint using the method of Lagrange multipliers because both the distortion function and the capacity function have continuous first partial derivatives on $(t_p, t_n) \in (0, \infty) \times (-\infty, 0)$. From this we get the optimal threshold must be satisfied by (5).

$$t_n + t_p + 1 = 0 \tag{5}$$

Let us consider the solution of the optimization problem (1). We see that the solution is the point common to two lines, the straight line (5) and the curve line found by putting the required payload (τ) into (4). Now we know that the exact solution of the optimization problem by plugging (5) into (4). However, the proposed method we present thereafter does not use it. The details will be given in the next section.

There are some differences found in the model [27] compared to our model. We note that $h(x)$ in our model is a little bit different from model [27] since the right side of the t_p threshold value is shifted by t_p+1 (a model [27] shifted by t_p), and the cost of distortion is of $(t_p+1)^2$. An advantage of this function, $h(x)$, is that its formula leads us to find a simple relation between optimal threshold values (5) which we can use to design our algorithm.

3. THE PROSED SCHEME

We want a method which is simple, does not require any extra tools, and helps us get optimal threshold values. To begin, we show the histogram applied on median edge detector (MED) prediction-errors [11] (solid line) and the Laplacian distribution model (dotted line) in Figure 1. Zhou and Au [27], the PE histogram is modeled by using a Laplacian distribution. Its shape parameter is an approximate average of absolute of PE values. Let us consider the histograms of Barbara and Airplane in Figures 1(a) and 1(b) respectively. We compare the Laplacian distribution model with the prediction-error histogram calculated by MED [11].

We see that the model is not suitable to simulate the actual histogram of Barbara and Airplane because their prediction-error distributions are not Laplacian. Embedding rate (BPP) versus the threshold values are shown in Figure 2. Consequently, a method [27] cannot achieve the optimal threshold values as can be seen in Figures 2(a) Lena, 2(b) Barbara, and 2(c) Airplane respectively. In our proposed method, we define an approximate capacity function corresponding to each of the threshold values directly from an image of actual data which is more accurate than the modelling function.

(a)   (b)
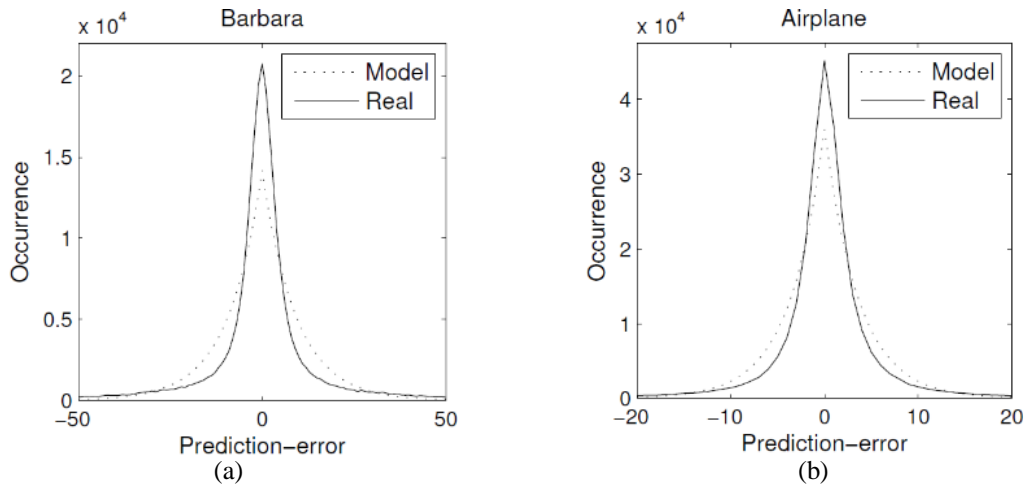
Figure 1. Histogram applied on MED prediction-errors [11] (solid line) and the Laplacian distribution model (dotted line) versions on (a) Barbara and (b) Airplane

(a)   (b)

(c)
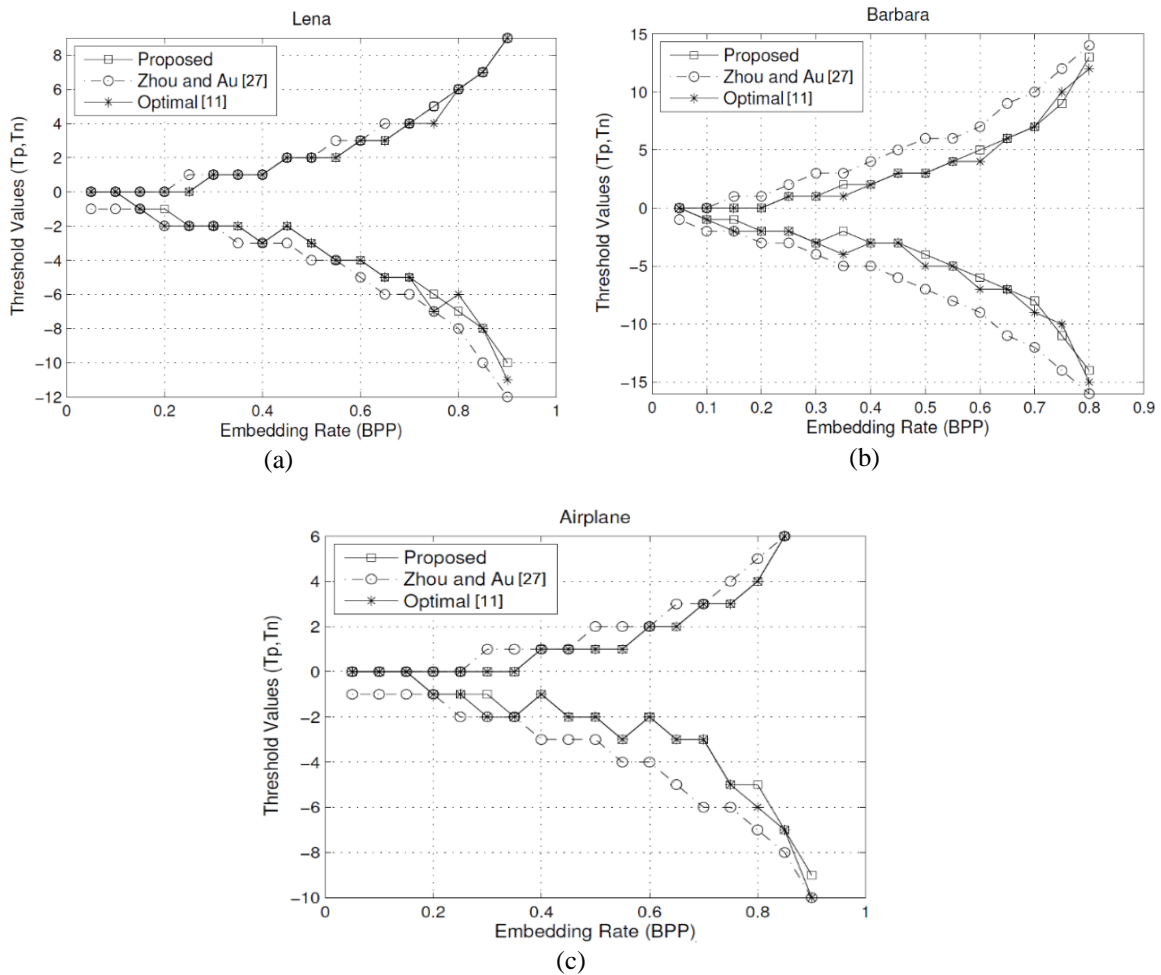
Figure 2. BPP versus the threshold values of our approach in comparison with [27] and the optimal threshold values obtained by complete search based on algorithm [11]. The test set is constituted of gray-scale image; (a) Lena, (b) Brabara, and (c) Airplane

As mentioned in the previous section, the threshold values should lie on a boundary of a constraint feasible region. In reality, we cannot obtain thresholds which exactly satisfy $C(T_p, T_n)=\tau$ because PE is discrete, however, the model PE is continuous. We attempt to get the values which are as close as possible to the boundary. Moreover, T_p and T_n must be satisfied by (5).

Our proposed method starts by creating a capacity function, $C(T_p, T_n)$, depending on two variables, T_p and T_n, from PE histogram information. The function values are a number of PE values lying in the range $[T_p, T_n]$ as an approximate embeddable payload. After the capacity function is defined, we construct a payload feasible region. Next, threshold values candidates are chosen by selecting the first k threshold values which are closest to the boundary ($C(T_p, T_n)=\tau$) and located on the feasible region. The optimal threshold values are sought from the candidates by calculating scores of all candidates using a score function (6).

$$S_i(T_p, T_n) = |T_n + T_p + 1| + k\hat{C}_i^k \tag{6}$$

where $i = 1,\ldots,k$. The range of the score function is a non-negative real number ($S_i(T_p, T_n) \in \mathbb{R} : S_i(T_p, T_n) \geq 0$). The symbol $|.|$ represents the absolute value. Here C_i^k is the normalized capacity value of the i-th candidate in a k-candidates set defined by (7).

$$\hat{C}_i^k = \left(\hat{C}_i^k(T_p, T_n) - \hat{C}_{min}^k(T_p, T_n)\right) / \left(\hat{C}_{max}^k(T_p, T_n) - \hat{C}_{min}^k(T_p, T_n)\right) \tag{7}$$

where C_{max}^k and C_{min}^k are maximum and minimum capacity values in a k-candidates set respectively. There are two significant terms involved in the score function. It is easy to see that the first term is the scaling distance from the line (5) to a feasible point, and max-min normalization is used to scale the capacity of candidates in second term, so that both terms could be compared relevantly. The score function is designed to be highest when thresholds capacity is closest to the required payload and satisfy the condition $T_n+T_p+1=0$. Its value decays when threshold positions are far away from the conditions. We consider a candidate with the highest score as having the optimal threshold approximated values.

Our proposed algorithm is summarized as follows:
a) Build a capacity function from PE histogram and define a constraint feasible region.
b) Select candidates from the first k closet-to-boundary threshold values from the feasible region.
c) Calculate candidates' score.
d) Select the candidate that earns the highest score as a set of approximated optimal threshold values.

4. EXPERIMENTAL RESULTS

Our method was applied to three natural standard 512×512 sized 8-bits gray scale images Lena, Barbara and Airplane, used as reference in the literature. The three test images downloaded from http://sipi.usc.edu/database. The number of candidates, k, is 25 in our implementation. We compared our method with the scheme proposed in [27] and the optimal threshold values obtained by complete search based on algorithm [11] as can be seen in Figure 2(a) Lena, 2(b) Brabara, and 2(c) Airplane. Our method provides closer optimal threshold values than method [27]. For example, in the Barbara image, the distribution of the prediction error is not Laplacian, which extremely affects and reduces the accuracy of the capacity estimation given in method [27], but this does not happen in our method because it is independent of the Laplacian distribution modelling. In particular, the results in Figure 2(b) show that their T_p and T_n values are far from the optimal threshold values. In this way, our method yields a superior performance to methods [27] for all images.

To achieve the best threshold values for the embedding algorithm, it requires a few more iteration steps from the approximated optimal threshold values to the actual one. In our method, there exists threshold candidates which are located close to the payload constraint boundary. From this implementation, the exact optimal parameters always involve in this group of candidates. It is obvious that the score for the correct optimal threshold is normally low. So after the set of approximated threshold values is defined, we searched for the optimal parameters sequenced by threshold score in ascending order. The optimal threshold values are mostly achieved in the first four iterations. In Figure 3, the bar charts represent the number of iterations required to obtain the optimal threshold values. Furthermore, Figures 3(a) to 3(c) presents a number of iterations used to find the correct optimal thresholds relying on [11], [27] the proposed method for imaging Lena, Barbara and Airplane. Notice that the proposed method finds the best threshold values the first time in the search.
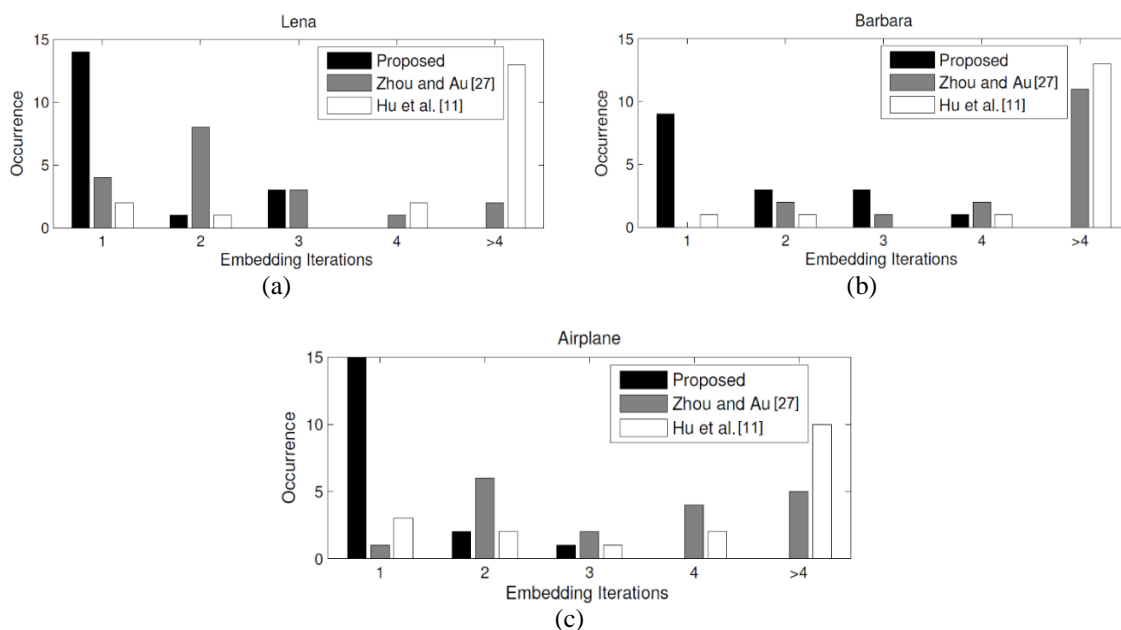
Figure 3. Bar charts represent the number of iterations required to obtain the optimal threshold values by using [11], [27] and the proposed method for image Lena; (a) Barbara, (b) Airplane, and (c) Respectively

5. CONCLUSION

The main aim of this work is to find a simple method for determining an optimal threshold values used in histogram shifting technique. Performance of optimal threshold determining technique cost less than fine-tuning iteration method which sometimes cannot find the optimal one. The main idea of the proposed scheme is to use a score function. This is derived from the optimal threshold properties as a feature to predict the correct optimum. There is no doubt that implementing these results, shows that the algorithm has superior performance. It could select a closer threshold values to the correct optimal threshold values. It also requires less time to obtain the satisfactory parameter values without additional tools.

REFERENCES

[1]   M. U. Celik, G. Sharma, A. M. Tekalp, and E. Saber, "Reversible data hiding," in *In Proceedings. International Conference on Image Processing*, vol. 2, pp. 157–160, 2002.
[2]   J. Fridrich, M. Goljan, and R. Du, "Invertible authentication," *in Procedding SPIE Security Watermarking Multimedia Contents*, vol. 4314, pp. 197–208, 2021.
[3]   G. Xuan, J. Zhu, J. Chen, Y. Q. Shi, Z. Ni, and W. Su, "Distortionless data hiding based on integer wavelet transform," *Electronics Letters*, vol. 38, no. 25, pp. 1646–1648, 2002, doi: 10.1049/el:20021131.
[4]   G. Xuan, C. Yang, Y. Zhen, Y. Q. Shi, and Z. Ni, "Reversible data hiding using integer wavelet transform and companding technique," in *Lecture Notes in Computer Science*, vol. 3304, Springer Berlin Heidelberg, 2005, pp. 115–124.
[5]   G. Xuan *et al.*, "High capacity lossless data hiding based on integer wavelet transform," in *Proceedings - IEEE International Symposium on Circuits and Systems*, 2004, vol. 2, doi: 10.1109/iscas.2004.1329200.
[6]   G. Xuan, Y. Q. Shi, C. Yang, Y. Zheng, D. Zou, and P. Chai, "Lossless data hiding using integer wavelet transform and threshold embedding technique," in *IEEE International Conference on Multimedia and Expo, ICME 2005*, 2005, vol. 2005, pp. 1520–1523, doi: 10.1109/ICME.2005.1521722.
[7]   G. Xuan *et al.*, "Lossless data hiding using histogram shifting method based on integer wavelets," in *Lecture Notes in Computer Science (including subseries Lecture Notes in Artificial Intelligence and Lecture Notes in Bioinformatics)*, vol. 4283 LNCS, Springer Berlin Heidelberg, 2006, pp. 323–332.
[8]   J. Tian, "Reversible data embedding using a difference expansion," *IEEE Transactions on Circuits and Systems for Video Technology*, vol. 13, no. 8, pp. 890–896, Aug. 2003, doi: 10.1109/TCSVT.2003.815962.
[9]   A. M. Alattar, "Reversible watermark using the difference expansion of a generalized integer transform," *IEEE Transactions on Image Processing*, vol. 13, no. 8, pp. 1147–1156, Aug. 2004, doi: 10.1109/TIP.2004.828418.
[10]   Y. Hu, H. K. Lee, K. Chen, and J. Li, "Difference expansion based reversible data hiding using two embedding directions," *IEEE Transactions on Multimedia*, vol. 10, no. 8, pp. 1500–1512, Dec. 2008, doi: 10.1109/TMM.2007341.
[11]   Y. Hu, H. K. Lee, and J. Li, "DE-based reversible data hiding with improved overflow location map," *IEEE Transactions on Circuits and Systems for Video Technology*, vol. 19, no. 2, pp. 250–260, Feb. 2009, doi: 10.1109/TCSVT.2008.2009252.

[12] H. C. Huang, F. C. Chang, and W. C. Fang, "Reversible data hiding with histogram-based difference expansion for QR code applications," *IEEE Transactions on Consumer Electronics*, vol. 57, no. 2, pp. 779–787, May 2011, doi: 10.1109/TCE.2011.5955222.

[13] H. J. Kim, V. Sachnev, Y. Q. Shi, J. Nam, and H. G. Choo, "A novel difference expansion transform for reversible data embedding," *IEEE Transactions on Information Forensics and Security*, vol. 3, no. 3, pp. 456–465, Sep. 2008, doi: 10.1109/TIFS.2008.924600.

[14] L. Kamstra and H. J. A. M. Heijmans, "Reversible data embedding into images using wavelet techniques and sorting," *IEEE Transactions on Image Processing*, vol. 14, no. 12, pp. 2082–2090, Dec. 2005, doi: 10.1109/TIP.2005.859373.

[15] V. Sachnev, H. J. Kim, J. Nam, S. Suresh, and Y. Q. Shi, "Reversible watermarking algorithm using sorting and prediction," *IEEE Transactions on Circuits and Systems for Video Technology*, vol. 19, no. 7, pp. 989–999, Jul. 2009, doi: 10.1109/TCSVT.2009.2020257.

[16] K. Edris, J. M. Zain, and T. A. A. Kadir, "Reversible watermarking based on sorting prediction algorithm," *International Journal of Computer Systems & Software Engineering*, vol. 1, no. 1, pp. 119–129, Feb. 2015, doi: 10.15282/ijsecs.1.2015.10.00010.

[17] X. Li, B. Yang, and T. Zeng, "Efficient reversible watermarking based on adaptive prediction-error expansion and pixel selection," *IEEE Transactions on Image Processing*, vol. 20, no. 12, pp. 3524–3533, Dec. 2011, doi: 10.1109/TIP.2011.2150233.

[18] J. Xu, H. Zhou, W. Zhang, R. Jiang, G. Ma, and N. Yu, "Second order perdicting-error sorting for reversible data hiding," in *Lecture Notes in Computer Science (including subseries Lecture Notes in Artificial Intelligence and Lecture Notes in Bioinformatics)*, vol. 10082 LNCS, Springer International Publishing, 2017, pp. 407–420.

[19] C. Panyindee, "Improved rhombus predictor for reversible data hiding based on PEHS and sorting using linear weight fitting," *Naresuan University Engineering Journal*, vol. 14, no. 1, pp. 50–60, 2019.

[20] H. J. Hwang, "Reversible watermarking method using optimal histogram pair shifting based on prediction and sorting," *KSII Transactions on Internet and Information Systems*, 2010, doi: 10.3837/tiis.2010.08.012.

[21] A. Kotvicha, P. Sanguansat, and M. L. K. Kasemsa, "Expand variance mean sorting for reversible watermarking," *International Journal of Computer and Communication Engineering*, pp. 196–199, 2012, doi: 10.7763/ijcce.2012.v1.51.

[22] S. U. Kang, H. J. Hwang, and H. J. Kim, "Reversible watermark using an accurate predictor and sorter based on payload balancing," *ETRI Journal*, vol. 34, no. 3, pp. 410–420, Jun. 2012, doi: 10.4218/etrij.12.0111.0075.

[23] M. Afsharizadeh and M. Mohammadi, "A reversible watermarking prediction based scheme using a new sorting technique," *Proceedings of the International MultiConference of Engineers and Computer Scientists,* 2013, doi: 10.1109/ISCISC.2013.6767347.

[24] C. Panyindee, "Appropriate variance mean for sorting based on a reversible watermarking algorithm," *Proceedings of the International MultiConference of Engineers and Computer Scientists*, vol. 1, pp. 345–348, 2016.

[25] D. M. Thod and J. J. Rodríguez, "Prediction-error based reversible watermarking," in *Proceedings - International Conference on Image Processing, ICIP*, 2004, vol. 3, pp. 1549–1552, doi: 10.1109/ICIP.2004.1421361.

[26] D. M. Thodi and J. J. Rodríguez, "Expansion embedding techniques for reversible watermarking," *IEEE Transactions on Image Processing*, vol. 16, no. 3, pp. 721–730, Mar. 2007, doi: 10.1109/TIP.2006.891046.

[27] J. Zhou and O. C. Au, "Determining the capacity parameters in PEE-Based reversible image watermarking," *IEEE Signal Processing Letters*, vol. 19, no. 5, pp. 287–290, May 2012, doi: 10.1109/LSP.2012.2190508.

[28] B. Ou, X. Li, Y. Zhao, R. Ni, and Y. Q. Shi, "Pairwise prediction-error expansion for efficient reversible data hiding," *IEEE Transactions on Image Processing*, vol. 22, no. 12, pp. 5010–5021, Dec. 2013, doi: 10.1109/TIP.2013.2281422.

[29] X. Li, J. Li, B. Li, and B. Yang, "High-fidelity reversible data hiding scheme based on pixel-value-ordering and prediction-error expansion," *Signal Processing*, vol. 93, no. 1, pp. 198–205, Jan. 2013, doi: 10.1016/j.sigpro.2012.07.025.

[30] I. C. Dragoi and D. Coltuc, "Local-prediction-based difference expansion reversible watermarking," *IEEE Transactions on Image Processing*, vol. 23, no. 4, pp. 1779–1790, Apr. 2014, doi: 10.1109/TIP.2014.2307482.

[31] C. Yu, X. Zhang, D. Wang, and Z. Tang, "Reversible data hiding with pairwise PEE and 2D-PEH decomposition," *Signal Processing*, vol. 196, p. 108527, Jul. 2022, doi: 10.1016/j.sigpro.2022.108527.

[32] R. Hu and S. Xiang, "Reversible data hiding by using CNN prediction and adaptive embedding," *IEEE Transactions on Pattern Analysis and Machine Intelligence*, vol. 44, no. 12, pp. 10196–10208, Dec. 2022, doi: 10.1109/TPAMI.2021.3131250.

[33] X. Wang, X. Wang, B. Ma, Q. Li, and Y. Q. Shi, "High precision error prediction algorithm based on ridge regression predictor for reversible data hiding," *IEEE Signal Processing Letters*, vol. 28, pp. 1125–1129, 2021, doi: 10.1109/LSP.2021.3080181.

[34] Z. Ni, Y. Q. Shi, N. Ansari, and W. Su, "Reversible data hiding," *IEEE Transactions on Circuits and Systems for Video Technology*, vol. 16, no. 3, pp. 354–361, Mar. 2006, doi: 10.1109/TCSVT.2006.869964.

[35] G. Coatrieux, C. Le Guillou, J. M. Cauvin, and C. Roux, "Reversible watermarking for knowledge digest embedding and reliability control in medical images," *IEEE Transactions on Information Technology in Biomedicine*, vol. 13, no. 2, pp. 158–165, Mar. 2009, doi: 10.1109/TITB.2008.2007199.

[36] D. Coltuc, "Improved embedding for prediction-based reversible watermarking," *IEEE Transactions on Information Forensics and Security*, vol. 6, no. 3 PART 2, pp. 873–882, Sep. 2011, doi: 10.1109/TIFS.2011.2145372.

[37] S. Boyd and L. Vandenberghe, *Convex optimization*. Cambridge University Press, 2004.

BIOGRAPHIES OF AUTHORS

Chaiyaporn Panyindee (iD) (g) (SC) (◐) is Assistant Professor at Department of Computer Engineering, Faculty of Engineering, Rajamangala University of Technology Rattanakosin, Thailand. He Holds a Ding D.Eng degree in Electrical Engineering with specialization in data hiding. He is director of Image Processing Research Lab. His research interests include image processing, data hiding, medical image analysis, and pattern recognition. He can be contacted at email: Chaiyaporn.pan@rmutr.ac.th.